I&EC research
Industrial & Engineering Chemistry Research

Article

Cite This: Ind. Eng. Chem. Res. 2018, 57, 8802−8809

pubs.acs.org/IECR

Influence of Feed-Electrode Concentration Differences in Flow-Electrode Systems for Capacitive Deionization

Daniel Moreno and Marta C. Hatzell*

Department of Mechanical Engineering, Georgia Institute of Technology, Atlanta, Georgia 30332-0405, United States

Supporting Information

ABSTRACT: The common performance metrics ascribed to flow electrode capacitive deionization systems can vary significantly depending on the mode of operation and initial system conditions. Through varying the flow electrolyte ionic strength, performance values such as average salt adsorption rate and energy consumption can vary by as much as 51 and 55%. This variability from cycle to cycle is in part due to changes in the electrical conductivity (ohmic) but is also due to the introduction of competing transport processes. Diffusive transport can enhance or diminish the rate of desalination and energy recovery, creating a larger degree of error in reported values. Here, we propose a dimensionless ratio comparing diffusion and electromigration-based transport to measure performance stability. Unstable system performance is most prominent when the feed ionic strength does not match the flow electrode ionic strength. In this scenario, the ratio of the diffusion to electromigration transport reached a maximum. Conversely, stable operation occurs when the ionic strength of the feed matches the ionic strength in the flow electrode. With the growing interest to move flow electrode capacitive deionization into treatment regimens which operated with high concentration feedwater, characterizing and quantifying diffusive flux is important for assessing true electrochemical system performance.

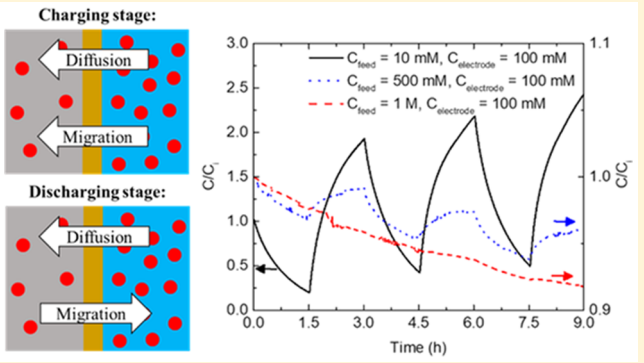

1. INTRODUCTION

Capacitive deionization (CDI) has shown promise for treating brackish waters.[1] The low projected cost and antifouling surfaces provide valuable advantages when compared with state of the art technologies such as reverse osmosis (RO)[2] and flash stage distillation.[3] CDI is limited to low saline solutions as traditional film electrodes have a finite surface area available for ion removal. Flow electrode capacitive deionization (FCDI) overcomes this limitation through transforming the static electrodes into flow electrodes, which are stored in tanks outside of the flow cell. This allows for much higher surface area per flow cell volume, permitting the treatment of higher saline waters (e.g., seawater).

The flow electrode consists of solid active material (activated carbon) mixed with a salt-based electrolyte. To date, most efforts aim to improve system performance through evaluating new materials, system configurations, and innovative ways to increase carbon loading in the electrode.[4−7] The flow electrode-supporting electrolyte has received less attention with the majority of researchers using various concentrations (0−0.5 M) of sodium chloride.[2,5−11] Increasing the salt concentration reduces the whole cell solution ohmic resistance and consequently can improve the electrochemical cell performance. Yet, increasing the ionic strength has been shown to increase the desalination efficiency only up until ∼0.4 M sodium chloride (E_{cell} < 1.2 V) and decreases beyond this point.[12] Higher saline electrolytes (0.5 M $NaSO_4$) were observed to improve the rate of desalination only at elevated voltages (E_{cell} > 1.5 V), but side reactions at these voltages can limit charge efficiency. Varying the electrolyte and feed ionic concentration also has a significant impact of membrane ionic resistance, which ultimately can limit system performance.[13−17] Thus, understanding and quantifying all transport-based processes occurring between the electrode and electrolyte will aid in overcoming performance limitations.

Here, we investigate the ability to obtain stable performance metrics (desalination and energy recovery) in a FCDI. We evaluate the interactions between the feed and the electrode by quantifying the charge efficiency, salt removal efficiency, energy input, and average salt adsorption rate during a series of charge−discharge cycles. In addition, we develop a transport model that decouples and quantitatively compares the various modes of ion transport (diffusion and migration) with a dimensionless ratio. This ratio is able to serve as a predictive measure for reporting the degree of stability within a given electrochemical FCDI performance measurement.

Received: April 14, 2018
Revised: June 6, 2018
Accepted: June 6, 2018
Published: June 6, 2018

DOI: 10.1021/acs.iecr.8b01626
Ind. Eng. Chem. Res. 2018, 57, 8802−8809

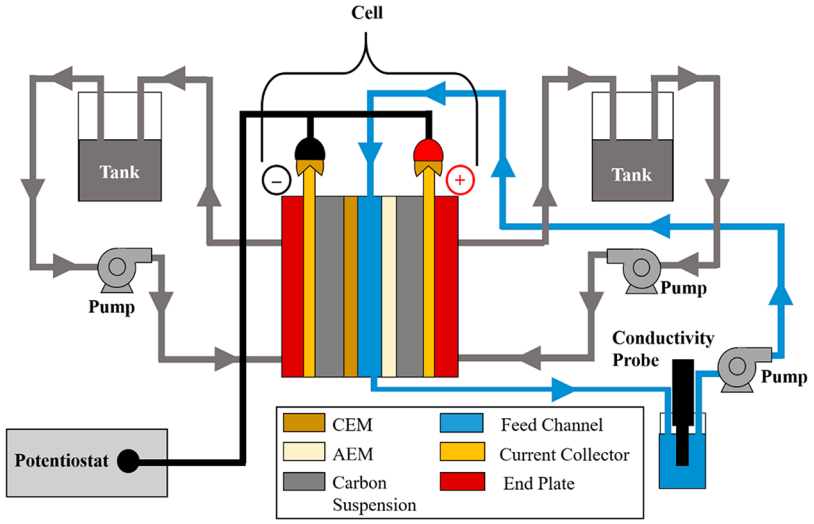

Figure 1. Schematic of FCDI cell setup.

2. MATERIALS AND METHODS

The FCDI system is comprised of a Model 857 Redox Flow Cell Test System (Figure 1) (Scribner Associates, Inc., Southern Pines, North Carolina) (Figure 1). Tanks for the flow electrode contain stir plates to enable continuous mixing of the electrode during testing. The flow cell (area A_{cell} = 25 cm^2) contains a polycarbonate flow channel (clear polycarbonate, 0.47 cm thickness) and gold-plated copper current collectors. The carbon slurries flow through two graphite plates with channels (1 mm width × 5 cm length × 1 mm depth, 33 channels total in a triple serpentine flow pattern), and the feed flows vertically through the center of the cell. Cation exchange membranes (CEM) and anion exchange membranes (AEM) separate the feed from electrode (Selemion AMV/CMV, Chiba, Japan).

The feed and electrode flow rates used during the experiment were 5 and 10 mL/min. The flow electrode (100 mL) consisted of 5 wt % activated charcoal Norit (Sigma-Aldrich, St. Louis, Missouri) with a variable concentration of sodium chloride salt (Sigma-Aldrich, St. Louis, Missouri, ACS reagent, ≥99%). The feed (25 mL) was prepared with three different salt concentrations: 10 mM, 500 mM, and 1 M. The cell was charged and discharged for 1.5 h at a voltage of 1.2 V to limit water splitting.[12] The feed conductivity was measured using an Orion Fisher Scientific 013005MD Versa Star Pro Benchtop conductivity meter, and the current through the cell was collected from the Flow Cell software. The data obtained for conductivity and current were used as inputs for the transport-based model.

The average salt adsorption rate (ASAR) was calculated to determine overall salt removal during each of the cycles:

$$\mathrm{ASAR} = \frac{\int_0^T (C_\mathrm{i} - C_\mathrm{f})\mathrm{d}t\Phi_f M_{\mathrm{NaCl}}}{m_{\mathrm{AC}}t} \tag{1}$$

where C_f is the feed concentration at any given time, C_i is the initial concentration in the feed, Φ_f is the feed flow rate, M_{NaCl} is the molar mass of NaCl, m_{AC} is the total mass of activated carbon in both electrodes, and t is time. Charge efficiency (CE) was calculated to determine salt removal in relation to energy input during charging stage:[18−20]

$$\mathrm{CE} = \frac{(C_{\mathrm{f,i}} - C_{\mathrm{f,f}})V_\mathrm{f}F}{\int_0^T I\mathrm{d}t} \tag{2}$$

where $C_{f,i}$ represents the initial concentration in the feed, $C_{f,f}$ represents the final concentration in the feed, V_f is the feed volume, I is the current, F is Faraday's constant, and t is the time. The salt removal efficiency (SRE) was calculated using the following:

$$\mathrm{SRE} = \frac{(C_{\mathrm{f,i}} - C_{\mathrm{f,f}})}{C_{\mathrm{f,i}}} \tag{3}$$

The study considered six different cases for feed and electrolyte concentrations. Three feed concentrations are examined: a dilute feed solution (10 mM), a moderate saline solution that was an approximate for seawater (0.5 M), and high concentration (1 M) which was meant to approximate a modest brine stream. In all of the matched tests, the electrode electrolyte concentration used was equivalent to that of the electrode electrolyte. In the mismatched tests, the electrode electrolyte concentration was fixed (100 mM), while the feed was varied. FCDI testing was conducted in a batch mode to discern the degree of reversibility between cycles.[7,21−28]

3. THEORY

The diffusion−migration ratio (DMR) was developed using the Nernst−Planck equation[29,30]

$$\frac{\partial C_i}{\partial t} = -\nabla N_i \tag{4}$$

where C_i represents cell concentration and N represents the flux. The subscript i describes the ith species (e.g Cl^- or Na^+). The flux, N_i, includes migration, diffusion, and convection terms:

$$N_i = -zu_iFC_i\nabla\varphi_i - D_\mathrm{i}\nabla C_i + C_\mathrm{i}v \tag{5}$$

where D_i is the diffusivity of ions in the feed. The diffusivity in the feed and electrolyte was approximated to be the same because the major component in both chambers was saline water. ∇C_i is the concentration gradient across the membrane, z is the ion valence, u_i is the ionic mobility, and $\nabla\varphi_i$ is the

DOI: 10.1021/acs.iecr.8b01626
Ind. Eng. Chem. Res. 2018, 57, 8802−8809

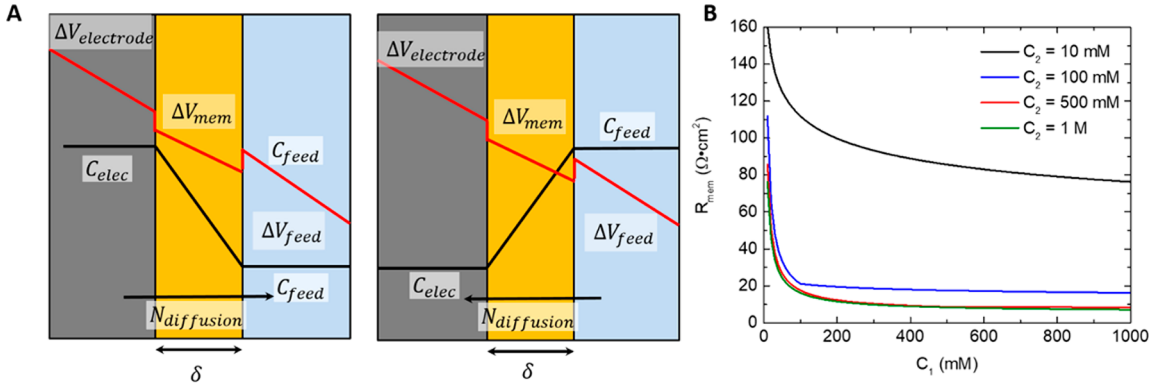

Figure 2. (A) Schematic depicting concentration and voltage drops across the membrane. (B) Variations in predicted membrane resistance as a function of varying concentrations in both the feed and the electrode.

potential gradient across the membrane. The ionic mobility u_i can also be expressed as $u_i = D_i/RT$.

With this 1-D model, the ratio of the diffusion to electromigration can be written as

$$\mathrm{DMR} \Rightarrow \frac{|N_{\mathrm{diffusion}}|}{|N_{\mathrm{migration}}|} \Rightarrow \frac{|-D_i \nabla C_i|}{|z u_i F C_i \nabla \varphi_i|} \Rightarrow \frac{\left|RT\frac{\partial C}{\partial x}\right|}{\left|zFC_f\frac{\partial V}{\partial x}\right|} \tag{6}$$

where $N_{\mathrm{diffusion}}$ is the diffusion flux, $N_{\mathrm{migration}}$ is the electromigration flux, R is the universal gas constant, and T is the operating temperature.

The diffusion to migration ratio can be calculated using experimentally obtained data (e.g., current, voltage, and conductivity (concentration). In the model, we neglect convection as the magnitude of the fluid velocity is negligible compared to diffusion and electromigration. We also assume the 1-D field is symmetric. Ions electroadsorbed from the salt solution are stored in the activated carbon slurry rather than in bulk. Thus, the overall electrode electrolyte ionic strength experiences relatively little change during the experiment. This is unlike the feed solution that varies during the desalination test.

The concentration gradient used to estimate diffusive transport is the difference in concentration between electrode (C_e) and feed (C_f) over the membrane thickness, δ:

$$\frac{\partial C}{\partial x} = \frac{C_e - C_f}{\delta} \tag{7}$$

Similarly, the electromigrative term in eq 5 encompasses information regarding the ohmic drop across the membrane (Figure 2A). The ohmic drop varies in magnitude based on surrounding electrolyte and feed concentrations. The ohmic drop ΔV_{mem} also varies as a function of the current density of the membrane and the membrane's resistance:

$$\Delta V_{\mathrm{mem}} = iR''_{\mathrm{mem}} \tag{8}$$

where i is current density in A/cm^2, and R'' is the membrane's resistance in Ω·cm^2. Experiments conducted at constant voltage result in current density profiles for eq 8. An approximation for the membrane resistance is

$$R''_{\mathrm{mem}} = a + \frac{b}{\left(\frac{C_e}{C_{\mathrm{ref}}}\right)} \tag{9}$$

where C_{ref} is a reference concentration to nondimensionalize the electrolyte concentration C_e (C_{ref} = 1 M). To account for variable concentration on either side (henceforth referred to as C_e and C_f), the study considers a power-law profile for the concentration across the membrane and averages the local resistance over the membrane to obtain the total resistance:

$$C(x) = \min(C_e, C_f) + |C_e - C_f|\left(\frac{x}{\delta}\right)^n \tag{10}$$

$$R''_{\mathrm{mem}} = \frac{1}{\delta}\int_0^{\delta}\left(a + \frac{b}{\left(\frac{C_e(x)}{C_{\mathrm{ref}}}\right)}\right)\mathrm{d}x \tag{11}$$

The three fitting parameters (a, b, and n) are membrane dependent and obtained from ex situ membrane testing. Here, a = 5.59, b = 1.55, and n = 5.5 (C_f = 10 mM and C_e = 1 M). Membrane resistances calculated from eqs 10 and 11) demonstrated that especially large variations occur if the concentration of either of the feed or electrolyte is low (Figure 2B). This is consistent with prior ex situ membrane testing.[14] Generally, AMV resistances for Selemion membranes are lower than the CMV; here, we assume that the AEM is 80% of the CEM's resistance.[14,16,31]

In considering migration into the feed, the electromigration term in eq 5 simplifies to

$$N_{\mathrm{migration}} = \frac{D_i F}{RT} C_{\mathrm{feed}} \frac{iR''_{\mathrm{mem}}}{\delta} \tag{12}$$

Thus, when taking a ratio of diffusive and electromigrative fluxes, the diffusivity term and membrane thickness effectively cancels. The final expression for the diffusion−migration ratio (DMR) is

$$\mathrm{DMR} = \frac{|C_{\mathrm{electrode}} - C_{\mathrm{feed}}|}{\frac{F}{RT} C_{\mathrm{feed}} iR''_{\mathrm{mem}}} \tag{13}$$

where temperature, feed concentration, and current density are experimentally obtained. In-line measured conductivity is converted to concentration using a calibration curve (eq S8 in the Supporting Information). Further details are provided in the Supporting Information (eqs S1−S8).

4. RESULTS AND DISCUSSION

One of the primary advantages of electrochemical separations is the ability to target and remove the minority component

DOI: 10.1021/acs.iecr.8b01626
Ind. Eng. Chem. Res. 2018, 57, 8802−8809

(ions) rather than majority component (water) in a mixture. This ability to remove the ionic species can promote low energy water treatment through unique system operation. Low energy consumption is possible because one can have control over the composition of the produced water, and hence, complete desalination is not necessary. Desired separation is achievable through changing the charging voltage (current) or time (Figure 3). Control over produced water salinity is increasingly becoming important for water treatment, as energy consumption takes place during the post-treatment phase through the reintroduction of minerals. A certain degree of mineral composition is required to minimize corrosion and for taste. The introduction of minerals during post treatment processes also adds to the cost and complexity of a treatment system.

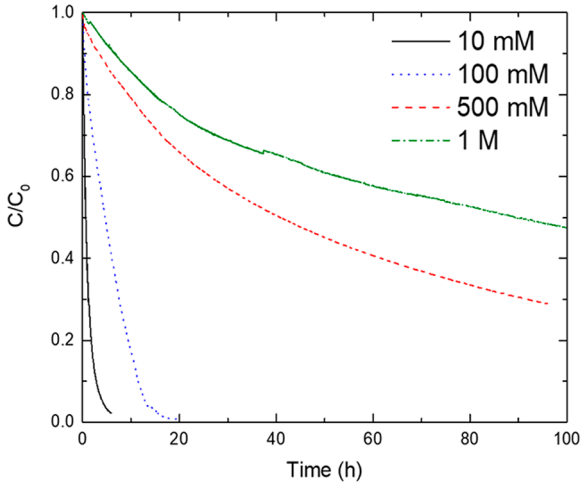

Figure 3. Flow electrodes can achieve various degrees of salt removal depending on the charging time, voltage and initial feed concentration.

This potential advantage associated with electrochemical-based separations technologies is important for FCDI systems that often operate with a range of feed solutions. For instance, a flow electrode with a modest carbon loading (5 wt %) is capable of achieving a range of exit salinities (Figure 3). With low saline feeds (10−100 mM), the percent of salt removed can easily be tuned from 0 to 100% by simply increasing the charge (desalination) time. This ability to control the exit salinity (or total salt removed) is most likely an even more favorable characteristic with higher concentration feed solutions. Here, the flexibility in exit salinity is also observed with a similar flow electrode (5 wt %), with total salt removed ranging from zero to 60% (C_{feed} = 0.5−1 M) (Figure 3), albeit at longer time scales. Therefore, a desalination test with an FCDI system would not necessarily operate solely to complete salt removal (C/C_0 = 0), but rather desalination would be cut off once a desired salinity is reached. This desalination process would correspond to the charging phase. Next, the electrodes could be regenerated and ideally returned to the initial state (C_e = $C_{e,i}$) using a discharge process. By returning the flow electrode ionic strength back to the initial condition, repeatable operation exists within the system.

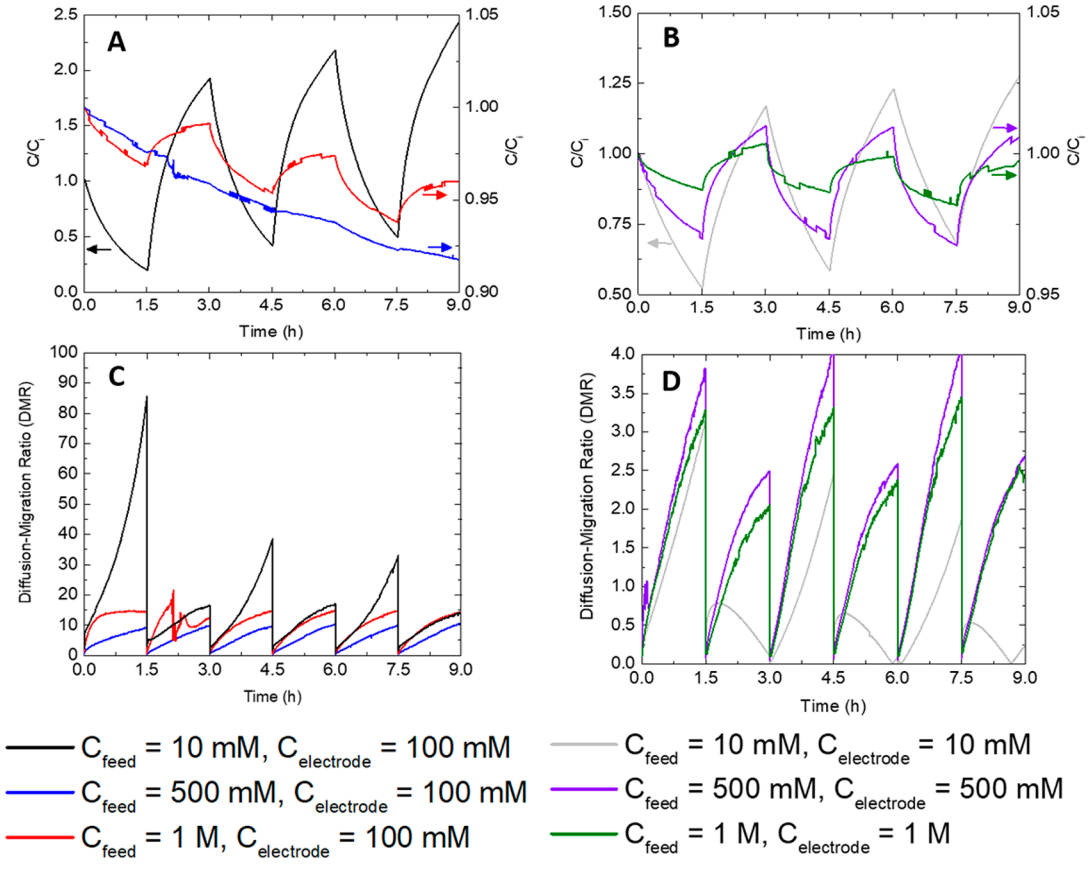

Figure 4. (A) Relative conductivity for mismatched feed and electrolyte, and (B) relative conductivity matching feed and electrolyte. (C) DMR for mismatched feed and electrolyte, and (D) DMR for matched feed and electrolytes.

DOI: 10.1021/acs.iecr.8b01626
Ind. Eng. Chem. Res. 2018, 57, 8802−8809

However, the complete reversal of a flow electrode back to the initial conditions is not always possible. For instance, when a flow electrode (5 wt % carbon in 100 mM NaCl) is operated with a range of feeds, there is a lack of reversibility observed from cycle to cycle during batch operation (Figure 4a). Completely reversible system performance would entail removing a certain number of ions from a feed and discharging the same number of ions into a brine. In addition, electrical reversibility would entail recovering during discharge the same number of electrons introduced during the charging phase. Graphically, reversible cycle-to-cycle performance occurs if the feed solution returns to the initial condition ($C/C_0 = 1$) after regeneration (discharge), and this did not occur in any test where the feed ionic strength was different than the electrode electrolyte ion concentration ($C_f \neq C_e$) (Figure 4a).

This lack of reversibility is not due to changes in electrochemical performance but to the presence of a concentration gradient between the feed and the electrode. This gradient causes a general trend whereby a portion of the ionic transport occurs via diffusive processes (Figure 4A, black line). This results in a greater degree of resalination per cycle than desalination. This excess resalination is exhibited by the feed increasing by nearly 2× following the first complete desalination−resalination (charge−discharge) process. Despite the overall increasing feed concentration, the total salt removed remained consistent at ∼75% notwithstanding the increasing initial feed concentration. The consistency in the total salt removed aligns with the fixed time scale and similar currents observed from cycle to cycle. The electrochemical performance was stable (repeatable) in each cycle (Figure S1). This indicates that attributing the increase in resalination is not due to an increase in current passing through the cell. Furthermore, the volume of each flow electrode and feed solutions did not change throughout the experiment, excluding effects such as leakage and/or osmotic transport. All tests were also conducted multiple times with various volume of flow electrodes (100, 300, and 500 mL). In each series of experiments, the observations remained the same (Figure S2).

When the concentration gradient was reversed ($C_f > C_e$), a decreasing trend was observed in the feed concentration post each desalination−resalination cycle (Figure 4A, red/blue lines). Therefore, in these tests, the degree of desalination was greater than the degree of resalination. This trend appears to be valuable as the ultimate goal of the technology is to remove ions through electrochemical forces. By removing ions through a diffusive transport process, the impact of electrochemical separations may be overestimated. This is important when trying to compare and access the practicality of a certain separations process for water treatment and when comparing results to predicted thermodynamic models.

When both the electrode and feed ionic strength matched ($C_f = C_e$), the cycle-to-cycle desalination stability increased significantly (Figure 4b). Maintaining the initial concentration after each cycle allowed for repeatable performance independent of the feed initial concentration (Figure 4B). A slight overshoot (increased resalination) did occur, but this is consistent with the notion that complete elimination of diffusive transport is impossible. Even with the ionic equilibrium at the start of the given experiment, the transient nature of the desalination process will bring the system away from an equilibrium. At this moment, diffusion may account for some ion transport. Therefore, diffusive transport is impossible to eliminate in an FCDI system, but limiting diffusion is imperative to enhance system stability.

In addition to maintaining repeatable charge−discharge desalination performance, there are numerous other benefits to operating FCDI in a stable near equilibrium regime. Operating at an equilibrium will allow for an increase in energy recovery and could enhance the rate of desalination. Thus, energy recovery improves, as any resalination that occurs through diffusion limits the number of ions that transport across the membranes for the sole purpose of balancing charge. It is still uncertain if energy recovery will be required within FCDI systems; however, if it is a desired characteristic, resalination must occur solely through electromigration. Enhancement in the rate of desalination is also probable, especially in the case where the feed solution is less saline than the electrolyte. In this scenario, the ion transport processes during desalination are in opposite directions (diffusion and electromigration), which may result in partial resalination during the desalination process.

Evaluation of the ratio of the observed diffusion to migration (DMR)-based transport can be a means to access the propensity for diffusion to play an active role during either the desalination and/or resalination process. During each process (desalination or resalination), the DMR increases with time and with an increase in the feed concentration (Figure 4C). As described above, an estimate of the electromigration-based transport is accomplished through the use of the 1-D-based model, where experimentally observed current density serves as the primary input. An estimate of the potential magnitude of diffusive-based transport uses the experimentally obtained feed concentration as the model input.

When the feed and electrode ionic strength differed ($C_f \neq C_e$), the DMR ratio ranged from 10 to 30 (Figure 4C). Conversely, during the matched experiments ($C_f = C_e$), DMR never exceeded four, and only approached this value at the end of a process, whereby the experiment is known not to be at an ionic equilibrium. The significance of the DMR reaching 30 (Figure 4C, black line) represents an electrochemical cell whereby the diffusive ionic transport is 30× greater than the electromigration-based transport. We do not anticipate that the diffusive transport is dominant across the ion-exchange membrane, yet when a large enough potential exists, the likelihood for partial transport through diffusion increases. In the matched experiments, the diffusive ionic transport only ever approached 4× that of electromigration. This low value promotes limited diffusive transport, and therefore nearly all observed ionic transport occurs through electromigration.

As stated above, this additional transport of ions through diffusion results in a direct reduction in energy recovery, and furthermore inhibits the system from achieving purely electrochemical separations. It should be noted that the total salt removed under the identical electrochemical conditions appears to be greater when $C_f \neq C_e$ rather than when $C_f = C_e$. Therefore, if the sole goal is the remove ions and reversible flow electrode performance is not required, the diffusive transport can appear as an advantageous effect. However, one should be careful to note the exact mode of separations (electrochemical and diffusive) when reporting performance values. Therefore, the DMR provides a means to assess if the performance can be attributed to electrochemical forces (e.g., electromigration) or if additional transport processes may play a role in mediating desalination or resalination. To mitigate

DOI: 10.1021/acs.iecr.8b01626
Ind. Eng. Chem. Res. 2018, 57, 8802−8809

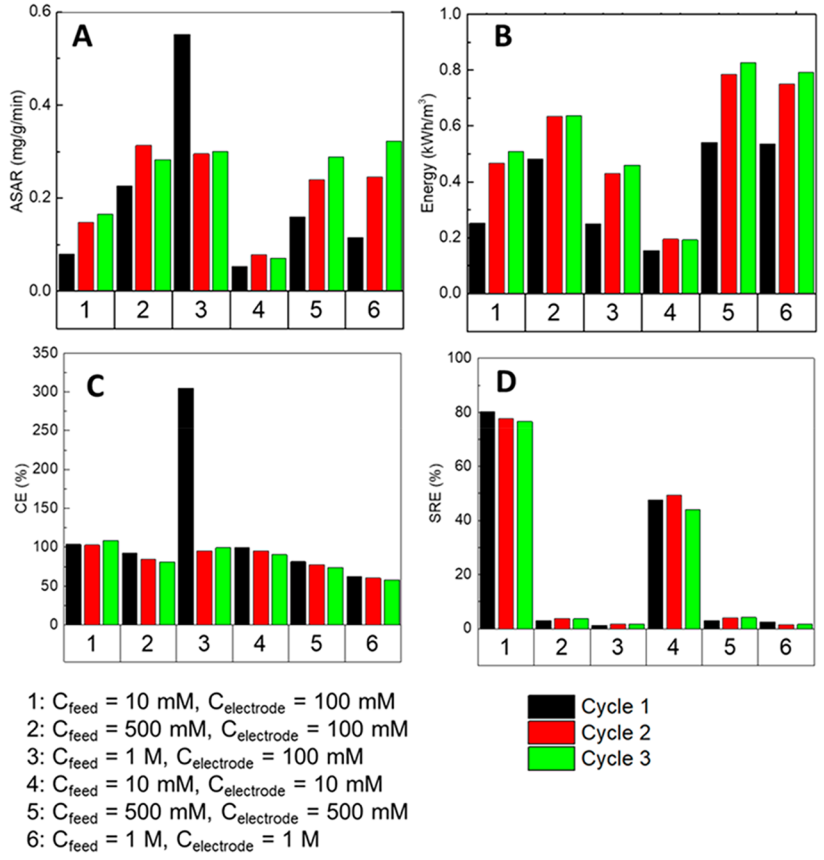

Figure 5. FCDI performance metrics: (A) ASAR, (B) energy consumed, (C) CE, and (D) SRE.

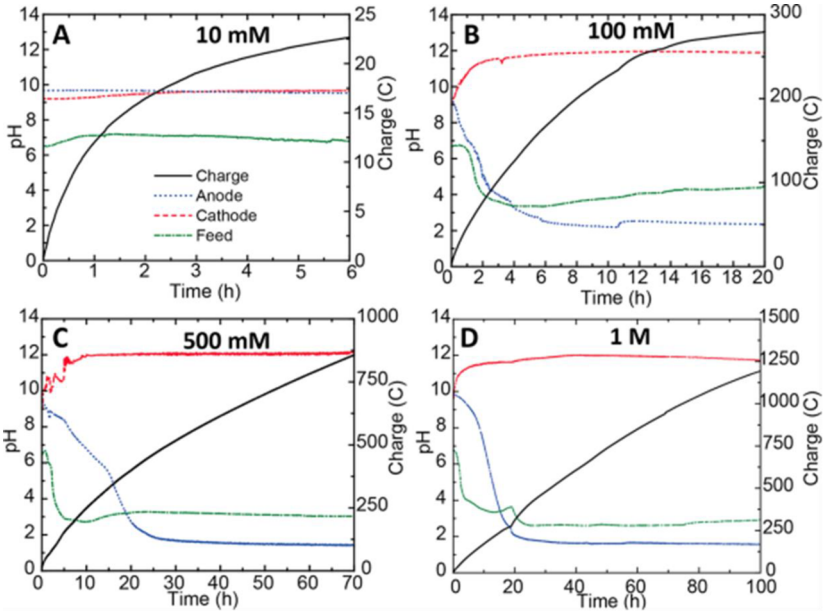

Figure 6. pH fluctuations and accumulated charge in the anode, cathode, and feed with (A) 10 mM feed, (B) 100 mM feed, (c) 500 mM feed, and (d) 1 M feed solutions.

any diffusive transport, we suggest operating and collecting performance metrics in cells where the DMR is less than five.

In addition to the diffusion effects associated with mismatched electrolyte and feed solutions, the concentration gradient across the membrane can alter the resistance of the membrane during operation. With a large gradient across the cell, resistance can vary tremendously, reaching a maximum of 600 $\Omega \cdot cm^2$ (Figure S3a) with the low concentration feed solution (10 mM). It is difficult to limit the resistance of a membrane in low saline solution, but the gradient across the membrane can exacerbate the resistance. For ideal electrochemical performance, whereby low energy consumption is required, membrane resistance should be low.

DOI: 10.1021/acs.iecr.8b01626
Ind. Eng. Chem. Res. 2018, 57, 8802−8809

The membrane resistance appears to decrease substantially when moving toward higher saline feed waters; however, in testing where the membrane was exposed to a gradient, the membrane resistance was almost 2× greater than that in testing with the ionic strengths matched (Figure S3b). In addition to reducing the membrane resistance, the variability in the membrane resistance decreases. Variable membrane resistance can contribute to a decrease in performance over time.

An additional consequence of the mismatched electrode and electrolyte ionic strength is the potential to overestimate system performance values. During testing with elevated DMR values where $C_f \neq C_e$, the ASAR was consistently greater than in testing with matched ionic strength $C_f = C_e$ (Figure 6A). The transport attributed to diffusion therefore overestimates the ASAR for the given electrochemical conditions. In particular, this is evident with the 1 M mismatch test, which displays by far the largest concentration difference between feed and electrode at the start of the cycle (ΔC = 900 mM). This led to both unusually high values for ASAR and CE (Figures 5A and C). In future cycles, as the system moves toward an equilibrium, the ASAR approaches a more reasonable value. When the cell moves away from an ionic equilibrium accentuated performance values can be obtained, but are not true measures of the electrochemical desalination performance. Due to the emerging nature of FCDI systems, there is a need for performance metrics that accurately depict the potential advantages or disadvantages of electrochemical-based separation technologies. For these tests, maintaining tests near ionic equilibrium will allow performance metrics to access the separations potential of FCDI.

Finally, in addition to ionic gradients within the flow electrode cell, there are large pH gradients that also can contribute to some of the performance variability. Generally, lower feed solutions (C_f = 10 mM) result in a negligible change in pH within the feed and/or electrolyte (Figure 6a), while larger saline feed solutions (C_f = 0.1−1 M) can result in a significant drop or rise in pH (Figures 6b−d). The change in pH correlates with the current or total charge that passes through the circuit. Side reactions, namely water splitting, are the source of the proton consumption and production and are hard to mitigate in a FCDI system operated with two electrodes. While the pH stabilizes, the pH change in the feed by as much as four to eight pH units can be disadvantageous for water treatment and membrane resistance and ultimately can also aid in moving the system away from an ionic equilibrium. The change in pH could therefore promote the transport of alternative ionic species (proton or hydroxide ions) transport rather than ionic species (Na^+ or Cl^-). Previous investigations have eliminated this pH gradient through recirculating the two flow electrodes in one reservoir, but this is at the expense of energy recovery.

The results obtained here offer some suggestions regarding the role variable ionic strength ($C_f \neq C_e$) plays on enhancing or diminishing long-term desalination performance within a FCDI system. The variable concentrations can exist due to experimental conditions or can arise through the production or consumption of protons due to side reactions. In either case, the impact is the addition of potential transport of ionic species through diffusion rather than purely electromigration-based transport. Because the ultimate goal with electrochemical separations is to move ions via electrochemical forces, diffusion should be limited. Matching the feed-electrolyte concentrations can mitigate this issue, but doing so requires greater energy input and limits the apparent salt removal.

CONCLUSION

Matching the ionic strength of the electrode and electrolyte to that of the feed promotes greater reliability in the reported desalination performance metrics (salt removal and ASAR, energy) in a FCDI system. For more dilute feeds, mismatched electrodes with a higher ion concentration can appear to improve desalination performance through minimizing ohmic resistances, but a gradual increase the feed solution is disadvantageous for promoting reversible system performance. When the feed concentration was much greater than that of the electrode, higher concentration gradients hindered the ability to recover salt into a waste stream, preventing full energy recovery. Therefore, characterizing the degree of diffusive transport between the feed and electrode is imperative for understanding and predicting the true electrochemical performance of FCDI systems. This will also become increasingly important as researchers move toward treating high saline solutions (seawater/produced) with FCDI systems.

ASSOCIATED CONTENT

Supporting Information

The Supporting Information is available free of charge on the ACS Publications website at DOI: 10.1021/acs.iecr.8b01626.

Additional details on experimental conditions, additional experimental performance data, long-term testing data, and experimentally observed resistance data (PDF)

AUTHOR INFORMATION

Corresponding Author

*E-mail: marta.hatzell@me.gatech.edu.

ORCID

Marta C. Hatzell: 0000-0002-5144-4969

Notes

The authors declare no competing financial interest.

ACKNOWLEDGMENTS

This material is based upon work supported by the National Science Foundation under Grant No. (1706290) for MCH. This work is also supported by the ARCS graduate fellowship to Daniel Moreno.

REFERENCES

(1) Zhang, J.; Hatzell, K. B.; Hatzell, M. C. A Combined Heat-and Power-Driven Membrane Capacitive Deionization System. *Environ. Sci. Technol. Lett.* **2017**, *4*, 470−474.

(2) Porada, S.; Zhao, R.; Van Der Wal, A.; Presser, V.; Biesheuvel, P. Review on the Science and Technology of Water Desalination by Capacitive Deionization. *Prog. Mater. Sci.* **2013**, *58*, 1388−1442.

(3) Anderson, M. A.; Cudero, A. L.; Palma, J. Capacitive Deionization as an Electrochemical Means of Saving Energy and Delivering Clean Water. Comparison to Present Desalination Practices: Will It Compete? *Electrochim. Acta* **2010**, *55*, 3845−3856.

(4) Cohen, H.; Eli, S. E.; Jõgi, M.; Suss, M. E. Suspension Electrodes Combining Slurries and Upflow Fluidized Beds. *ChemSusChem* **2016**, *9*, 3045−3048.

(5) Rommerskirchen, A.; Ohs, B.; Hepp, K. A.; Femmer, R.; Wessling, M. Modeling Continuous Flow-Electrode Capacitive Deionization Processes with Ion-Exchange Membranes. *J. Membr. Sci.* **2018**, *546*, 188−196.

DOI: 10.1021/acs.iecr.8b01626
Ind. Eng. Chem. Res. 2018, 57, 8802−8809

(6) Rommerskirchen, A.; Gendel, Y.; Wessling, M. Single Module Flow-Electrode Capacitive Deionization for Continuous Water Desalination. *Electrochem. Commun.* **2015**, *60*, 34−37.
(7) Gendel, Y.; Rommerskirchen, A. K. E.; David, O.; Wessling, M. Batch Mode and Continuous Desalination of Water Using Flowing Carbon Deionization (FCDI) Technology. *Electrochem. Commun.* **2014**, *46*, 152−156.
(8) Hatzell, K. B.; Boota, M.; Gogotsi, Y. Materials for Suspension (Semi-Solid) Electrodes for Energy and Water Technologies. *Chem. Soc. Rev.* **2015**, *44*, 8664−8687.
(9) Hatzell, K. B.; Hatzell, M. C.; Cook, K. M.; Boota, M.; Housel, G. M.; McBride, A.; Kumbur, E. C.; Gogotsi, Y. Effect of Oxidation of Carbon Material on Suspension Electrodes for Flow Electrode Capacitive Deionization. *Environ. Sci. Technol.* **2015**, *49*, 3040−3047.
(10) Hatzell, K. B.; Iwama, E.; Ferris, A.; Daffos, B.; Urita, K.; Tzedakis, T.; Chauvet, F.; Taberna, P.-L.; Gogotsi, Y.; Simon, P. Capacitive Deionization Concept Based on Suspension Electrodes Without Ion Exchange Membranes. Electrochem. *Electrochem. Commun.* **2014**, *43*, 18−21.
(11) Porada, S.; Weingarth, D.; Hamelers, H.; Bryjak, M.; Presser, V.; Biesheuvel, P. Carbon Flow Electrodes for Continuous Operation of Capacitive Deionization and Capacitive Mixing Energy Generation. *J. Mater. Chem. A* **2014**, *2*, 9313−9321.
(12) Liang, P.; Sun, X.; Bian, Y.; Zhang, H.; Yang, X.; Jiang, Y.; Liu, P.; Huang, X. Optimized Desalination Performance of High Voltage Flow-Electrode Capacitive Deionization by Adding Carbon Black in Flow-Electrode. *Desalination* **2017**, *420*, 63−69.
(13) Urano, K.; Masaki, Y.; Kawabata, M. Electric Resistances of Ion-Exchange Membranes in Dilute Solutions. *Desalination* **1986**, *58*, 171−176.
(14) Geise, G. M.; Curtis, A. J.; Hatzell, M. C.; Hickner, M. A.; Logan, B. E. Salt Concentration Differences Alter Membrane Resistance in Reverse Electrodialysis Stacks. *Environ. Sci. Technol. Lett.* **2014**, *1*, 36−39.
(15) Galama, A.; Vermaas, D.; Veerman, J.; Saakes, M.; Rijnaarts, H.; Post, J.; Nijmeijer, K. Membrane Resistance: The Effect of Salinity Gradients Over a Cation Exchange Membrane. *J. Membr. Sci.* **2014**, *467*, 279−291.
(16) Mir, F. Q.; Shukla, A. Sharp Rise in Resistance of Ion Exchange Membranes in Low Concentration NaCl Solution. *J. Taiwan Inst. Chem. Eng.* **2017**, *72*, 134−141.
(17) Choi, J.-H.; Kim, S.-H.; Moon, S.-H. Heterogeneity of Ion-Exchange Membranes: The Effects of Membrane Heterogeneity on Transport Properties. *J. Colloid Interface Sci.* **2001**, *241*, 120−126.
(18) Zhao, R.; Biesheuvel, P.; Van der Wal, A. Energy Consumption and Constant Current Operation in Membrane Capacitive Deionization. *Energy Environ. Sci.* **2012**, *5*, 9520−9527.
(19) Kim, T.; Dykstra, J.; Porada, S.; Van Der Wal, A.; Yoon, J.; Biesheuvel, P. Enhanced Charge Efficiency and Reduced Energy Use in Capacitive Deionization by Increasing the Discharge Voltage. *J. Colloid Interface Sci.* **2015**, *446*, 317−326.
(20) Hawks, S. A.; Knipe, J. M.; Campbell, P. G.; Loeb, C. K.; Hubert, M. A.; Santiago, J. G.; Stadermann, M. Quantifying the Flow Efficiency in Constant-Current Capacitive Deionization. *Water Res.* **2018**, *129*, 327−336.
(21) Linnartz, C. J.; Rommerskirchen, A.; Wessling, M.; Gendel, Y. Flow-Electrode Capacitive Deionization for Double Displacement Reactions. *ACS Sustainable Chem. Eng.* **2017**, *5*, 3906−3912.
(22) Cho, Y.; Lee, K. S.; Yang, S.; Choi, J.; Park, H.-r.; Kim, D. K. A Novel Three-Dimensional Desalination System Utilizing Honeycomb-Shaped Lattice Structures for Flow-Electrode Capacitive deionization. *Energy Environ. Sci.* **2017**, *10*, 1746−1750.
(23) Nativ, P.; Lahav, O.; Gendel, Y. Separation of Divalent and Monovalent Ions Using Flow-Electrode Capacitive Deionization with Nanofiltration Membranes. *Desalination* **2018**, *425*, 123−129.
(24) Nativ, P.; Badash, Y.; Gendel, Y. New Insights into the Mechanism of Flow-Electrode Capacitive Deionization. Electrochem. *Electrochem. Commun.* **2017**, *76*, 24−28.
(25) Luo, H.; Jenkins, P. E.; Ren, Z. Concurrent Desalination and Hydrogen Generation Using Microbial Electrolysis and Desalination Cells. *Environ. Sci. Technol.* **2011**, *45*, 340−344.
(26) Wang, M.; Huang, Z.-H.; Wang, L.; Wang, M.-X.; Kang, F.; Hou, H. Electrospun Ultrafine Carbon Fiber Webs for Electrochemical Capacitive Desalination. *New J. Chem.* **2010**, *34*, 1843−1845.
(27) Li, H.; Zou, L. Ion-Exchange Membrane Capacitive Deionization: A New Strategy for Brackish Water Desalination. *Desalination* **2011**, *275*, 62−66.
(28) Yuan, L.; Yang, X.; Liang, P.; Wang, L.; Huang, Z.-H.; Wei, J.; Huang, X. Capacitive Deionization Coupled with Microbial Fuel Cells to Desalinate Low-Concentration Salt Water. *Bioresour. Technol.* **2012**, *110*, 735−738.
(29) Bazant, M. Z.; Thornton, K.; Ajdari, A. Diffuse-Charge Dynamics in Electrochemical Systems. *Phys. Rev. E* **2004**, *70*, 021506.
(30) Biesheuvel, P.; Van Limpt, B.; Van der Wal, A. Dynamic Adsorption/Desorption Process Model for Capacitive Deionization. *J. Phys. Chem. C* **2009**, *113*, 5636−5640.
(31) Hassanvand, A.; Chen, G. Q.; Webley, P. A.; Kentish, S. E. Improvement of MCDI Operation and Design Through Experiment and Modelling: Regeneration with Brine and Optimum Residence Time. *Desalination* **2017**, *417*, 36−51.

DOI: 10.1021/acs.iecr.8b01626
Ind. Eng. Chem. Res. 2018, 57, 8802−8809